Inorg. Chem. **2008**, *47*, 4290−4298

Ammine Magnesium Borohydride Complex as a New Material for Hydrogen Storage: Structure and Properties of $Mg(BH_4)_2 \cdot 2NH_3$

Grigorii Soloveichik,*,† Jae-Hyuk Her,‡,§ Peter W. Stephens,‡ Yan Gao,† Job Rijssenbeek,† Matt Andrus,† and J.-C. Zhao†,||

General Electric Global Research Center, Niskayuna, New York 12309, and Department of Physics and Astronomy, Stony Brook University, Stony Brook, New York 11794

Received December 4, 2007

The ammonia complex of magnesium borohydride $Mg(BH_4)_2 \cdot 2NH_3$ (**I**), which contains 16.0 wt % hydrogen, is a potentially promising material for hydrogen storage. This complex was synthesized by thermal decomposition of a hexaaammine complex $Mg(BH_4)_2 \cdot 6NH_3$ (**II**), which crystallizes in the cubic space group $Fm\bar{3}m$ with unit cell parameter $a = 10.82(1)$ Å and is isostructural to $Mg(NH_3)_6Cl_2$. We solved the structure of **I** that crystallizes in the orthorhombic space group *Pcab* with unit cell parameters $a = 17.4872(4)$ Å, $b = 9.4132(2)$ Å, $c = 8.7304(2)$ Å, and $Z = 8$. This structure is built from individual pseudotetrahedral molecules $Mg(BH_4)_2 \cdot 2NH_3$ containing one bidentate BH_4 group and one tridentate BH_4 group that pack into a layered crystal structure mediated by N−H···H−B dihydrogen bonds. Complex **I** decomposes endothermically starting at 150 °C, with a maximum hydrogen release rate at 205 °C, which makes it competitive with ammonia borane BH_3NH_3 as a hydrogen storage material.

Introduction

Hydrogen storage is key in enabling technology for the proposed hydrogen economy, especially for vehicular applications. The U.S. Department of Energy has set targets for the year 2010 for hydrogen storage systems of 6 wt % for gravimetric capacity and 0.045 kg/L for volumetric capacity[1] that are very challenging. Taking into account that the ancillary components of the storage system (container, pumps, valves, etc.) account for about half of the total weight and volume, the material requirements are much higher, at least 12 wt % hydrogen. A few metal hydrides have such a capability. Many are not practical for use as hydrogen storage materials because they have hydrogen release temperatures that are too high [$LiBH_4$ (470 °C)[2] and $Mg(BH_4)_2$ (323 °C)[2]] or too low [$Ti(BH_4)_3$ (25 °C)[3]], are extremely dangerous because of high vapor pressure [$Be(BH_4)_2$ and $Al(BH_4)_3$], or are highly toxic [BeH_2, B_2H_6, and $Be(BH_4)_2$]. Systems based on hydrolysis of metal hydrides, e.g., $NaBH_4$, have a lower gravimetric capacity. Ammonia borane NH_3BH_3 would seem to be a promising hydrogen storage material, which potentially contains 19.6 wt % hydrogen. Hydrogen is irreversibly released from solid NH_3BH_3 by the recombination of protic (N−H) and hydridic (B−H) H atoms that are in close contact in the crystal (2.02 Å).[4] Thermal decomposition of solid NH_3BH_3 begins below 150 °C but gives only about 2 mol of H_2/1 mol of ammonia borane at practical temperatures (<500 °C), which corresponds to 13 wt % hydrogen.[5] Recently, catalyzed decomposition of ammonia borane was found to produce 2.5 mol of H_2 or 18 wt %.[6] However, this decomposition occurs in solution and requires 5 mol % of a heavy organometallic catalyst, thus substantially decreasing the practical hydrogen storage capacity. The hydrogen release from NH_3BH_3 is exothermic,[5] which makes

* To whom correspondence should be addressed. E-mail: soloveichik@crd.ge.com.
† General Electric Global Research Center.
‡ Stony Brook University.
§ Current address: Department of Materials Science and Engineering, University of Maryland, College Park, Maryland 20742-2115, and NIST Center for Neutron Research, National Institute of Standards and Technology, Gaithersburg, Maryland 20899-6102.
|| Current address: Materials Science and Engineering Department, Ohio State University, Columbus, Ohio 43210.

(1) Satyapal, S.; Petrovic, J.; Read, C.; Thomas, G.; Ordaz, G. *Catal. Today* **2007**, *120* (3−4), 246–256.
(2) Stasinevich, D. S.; Egorenko, G. A. *Zh. Neorg. Khim.* **1968**, *13* (3), 654–658.
(3) Volkov, V. V.; Myakishev, K. G. *Izv. Sib. Otd. Akad. Nauk SSSR, Ser. Khim. Nauk* **1977**, (1), 77–82.
(4) Klooster, W. T.; Koetzle, T. F.; Siegbahn, P. E. M.; Richardson, T. B.; Crabtree, R. H. *J. Am. Chem. Soc.* **1999**, *121* (27), 6337–6343.
(5) Baitalow, F.; Wolf, G.; Grolier, J. P. E.; Dan, F.; Randzio, S. L. *Thermochim. Acta* **2006**, *445* (2), 121–125.
(6) Keaton, R. J.; Blacquiere, J. M.; Baker, R. T. *J. Am. Chem. Soc.* **2007**, *129* (7), 1844–1845.

10.1021/ic7023633 CCC: $40.75
Published on Web 04/23/2008

controlled hydrogen release difficult and on-board regeneration highly unlikely. In addition, decomposition of ammonia borane also produces volatile compounds like ammonia and borazine $(HNBH)_3$ that reduce the hydrogen storage capacity and are harmful for polymer electrolyte membrane fuel cells.

To overcome some of the drawbacks of ammonia borane, we investigate the use of ammonia complexes of metal borohydrides $M(BH_4)_n \cdot mNH_3$ as a way of combining the properties of metal hydrides and ammonia borane. Such complexes are known to be stable at room temperature for Be, Mg, Ca, Zn, Cd, Al, Sc, Y, Ti, Zr, Cr, Co, and Ni.[7] Because ammonia is detrimental for many applications, the NH_3/BH_4 ratio (m/n) should presumably be equal to or less than unity. The most interesting of these is diammoniate of magnesium borohydride $Mg(BH_4)_2 \cdot 2NH_3$ having 16 wt % hydrogen. This complex was first described in 1985 by Konoplev and Silina.[8]

The starting material for the preparation of $Mg(BH_4)_2 \cdot 2NH_3$ is the hexaammine complex of magnesium borohydride $Mg(BH_4)_2 \cdot 6NH_3$, which has been known for almost 50 years.[9] This complex was first prepared by electrolysis of alkali-metal borohydrides with a magnesium anode in liquid ammonia.[9] This complex was subsequently prepared via several other pathways. Schultz and Parry[12a] and Plešek and Hermanek[12b] obtained the complex by an exchange reaction of magnesium thiocyanate with sodium borohydride in liquid ammonia. Huff et al.[10] claimed that $Mg(BH_4)_2 \cdot 6NH_3$ can be obtained by the displacement of sodium in $NaBH_4$ with magnesium metal in liquid ammonia in the presence of mercury. Konoplev et al.[10] reported that unsolvated magnesium borohydride forms the hexaammine complex when treated with ammonia at −70 °C. It has also been reported that dissolution of $Mg(BH_4)_2 \cdot 6HCONMe_2$ in liquid ammonia replaces dimethylformamide with ammonia, but the product was not fully characterized.[11] However, the purest $Mg(BH_4)_2 \cdot 6NH_3$ was obtained by the reaction of ammonia with a solution of $Mg(BH_4)_2$ etherate in ether at low temperature.[8,12,13]

The heating of hexaammoniate of magnesium borohydride at 118 °C in a vacuum for 4 h produced about 4 equiv of ammonia and the diammoniate complex $Mg(BH_4)_2 \cdot 2NH_3$.[8,12] However, the heating of $Mg(BH_4)_2 \cdot 6NH_3$ at ambient pressure cannot be stopped at this stage and leads to full decomposition.[8] The direct formation of diammoniate $Mg(BH_4)_2 \cdot 2NH_3$ and triammoniate $Mg(BH_4)_2 \cdot 3NH_3$ by treatment of a solution of magnesium borohydride in benzene and ether, respectively, was claimed,[14] but the stoichiometry of the product obtained in ether was not reproduced in later papers. Only the IR spectrum and thermogravimetric analysis data were reported for the diammoniate complex.[10] In this paper, we describe the synthesis, structure, and hydrogen release properties of $Mg(BH_4)_2 \cdot 2NH_3$.

Experimental Section

Materials and General Procedures. All experiments were performed under strictly anaerobic and anhydrous conditions by a a combination of standard Schlenk techniques and a Vacuum Atmospheres Nexus One glovebox filled with argon. The box atmosphere was maintained with less than 1 ppm of both O_2 and H_2O. Anhydrous diethyl ether, $NaBH_4$, and $MgCl_2$ with 95−99.8% purities were purchased from Sigma-Aldrich Co. Diethyl ether was then further dried using molecular sieves. Anhydrous ammonia gas (Air Products, 99.999%) was used as received.

Measurements. Elemental analyses were run on a Varian Liberty II inductively coupled plasma atomic emission spectrometer using a Sturman Master nebulizer and a Dionex model DX500 ion chromatograph. IR spectra of suspensions in mineral oil sealed between NaCl windows were recorded on a Nicolet Protégé 460 FT-IR spectrophotometer. Differential scanning calorimetry (DSC) analysis was done under a nitrogen purge using a TA Instruments 2920 differential scanning calorimeter. The samples were sealed into preweighed aluminum sample pans in the glovebox. The pan lids had 50 μm laser-drilled pinholes to allow ventilation of gaseous products. Volumetric temperature-programmed desorption (TPD) experiments were performed in a Sieverts type apparatus (PCTPro-2000 by Hy-Energy Scientific Instruments, LLC). A ∼200 mg sample was heated to 400 °C at a rate of 1 °C/min in a known volume initially under a vacuum. The pressure generated by the released hydrogen was then converted to H_2 (wt %) by the following formula:

$$H_2\ (\text{wt}\ \%) = \frac{\text{desorbed hydrogen}}{\text{initial weight of the sample}} \times 100$$

Attempts to recharge the dehydrogenated sample were made under 860 psi (5.9 MPa) of H_2 at 250 °C for up to 60 h.

Synthesis. Magnesium borohydride $Mg(BH_4)_2$ was prepared by interaction of $MgCl_2$ and $NaBH_4$ in diethyl ether (eq 1a) using an improved method described in the literature[15] and used without isolation.

$$MgCl_2 + 2NaBH_4 \rightarrow Mg(BH_4)_2 + 2NaCl \qquad (1a)$$

A 200 mL solution of 3.2 g of $Mg(BH_4)_2$ in Et_2O was placed into a two-neck, round-bottomed flask equipped with a gas inlet, a condenser, and a gas outlet. Anhydrous ammonia was passed through the cooled solution at a rate of about 40 mL/min (the cooling bath temperature was maintained below −10 °C) under vigorous stirring. White sediment formed almost immediately. After ∼10% excess ammonia was passed, the flow was stopped and the flask was allowed to warm up to room temperature. The solvent and remaining ammonia were removed in a vacuum to leave a white solid of composition $Mg(BH_4)_2 \cdot 6NH_3$ with an almost quantitative yield (8.86 g). Found: Mg, 14.94; B, 13.44 (the B/Mg ratio was 2.02). Calcd for $MgB_2N_6H_{26}$: Mg, 15.56; B, 13.84. Heating of the hexaammine complex of magnesium borohydride in a vacuum at 125 °C for 4 h caused noticeable expansion and partial melting of

(7) Kravchenko, O. V.; Kravchenko, S. E.; Semenenko, K. N. *Zh. Obshch. Khim.* **1990**, *60* (12), 2641–2660.
(8) Konoplev, V. N.; Silina, T. A. *Zh. Neorg. Khim.* **1985**, *30* (5), 1125–1128.
(9) Huff, G. F.; McElroy, A. D.; Adams, R. M. Electrochemical preparation of metal borohydrides. U.S. Patent 2,855,353, 1958.
(10) Konoplev, V. N.; Silina, T. A. 4th All-Union Conference on Chemistry of Hydrides, Dushanbe, Tajikstan, 1987; p 197.
(11) Mikheeva, V. I.; Konoplev, V. N. *Zh. Neorg. Khim.* **1965**, *10* (9), 2108–2114.
(12) (a) Schultz, D. R.; Parry, R. W. *J. Am. Chem. Soc.* **1958**, *80*, 4–8. (b) Plešek, J.; Hermanek, S. *Collect. Czech. Chem. Commun.* **1966**, *31* (10), 3845.
(13) Semenenko, K. N.; Shilkin, S. P.; Polyakova, V. B. *Izv. Akad. Nauk SSSR, Ser. Khim.* **1975**, (4), 735.
(14) Wagner, R. I.; Grant, L. R. Magnesium borohydride diammoniate and triammoniate. U.S. Patent 4,604,271, 1986.
(15) Konoplev, V. N. *Zh. Neorg. Khim.* **1980**, *25* (7), 1737–1740.

the starting material. The resulting colorless viscous liquid crystallized upon cooling as a white solid of composition $MgB_2N_2H_{14}$. Found: Mg, 25.95; B, 23.59 (the B:Mg ratio was 2.04). Calcd for $MgB_2N_2H_{14}$: Mg, 27.60; B, 24.55. The low numbers for the Mg and B contents compared to the theoretical values are probably because of incomplete decomposition of the hexaammine complex in the desolvation process.

Crystallography. For phase identification, samples were loaded into 0.5 mm glass capillaries inside the glovebox and sealed with vacuum grease for X-ray diffraction (XRD) measurement, using point-collimated Cu radiation (1.542 Å) with a graphite monochromator and an area detector (GADDS, Bruker-AXS, Inc.). The typical X-ray exposure time for a sample was 10 min.

In situ powder XRD was performed at the X7B Beamline of the National Synchrotron Light Source, Brookhaven National Laboratory. X-rays of $\lambda = 0.922$ Å were obtained from a Si(111) monochromator and were focused to 0.5 mm × 1 mm at the sample position by using a bent planar collimating mirror and a Rh-coated toroidal focusing mirror. The diffraction patterns were recorded with a Mar345 imaging plate detector and processed using the program *Fit2D*.[16] The time-resolved diffraction patterns were taken with $2\theta_{max} = 32°$ at a rate of one image per minute (20 s exposure and 40 s data readout time). The in situ sample cell used in the experiment has been previously described in detail.[17] The powder sample was loaded into a 0.5-mm-i.d. quartz capillary in an inert atmosphere glovebox, and the open end was sealed using vacuum grease. For measurement, the quartz capillary was opened just above the sample, quickly placed inside the sapphire tube of the cell, and immediately purged with flowing He. The total air exposure was usually less than 5 s. The sample was heated to 450 °C with a resistance heater, and the temperature was monitored with a chromel−alumel (K-type) thermocouple placed inside the sapphire capillary and touching the closed end of the sample capillary. During hydrogen desorption, the sample cell was connected to a residual gas analyzer (Stanford Research Systems RGA200) for real-time qualitative measurement of desorbed gases.

For structure determination, a high-resolution synchrotron powder diffraction pattern was collected at room temperature at the X16C Beamline of the National Synchrotron Light Source, Brookhaven National Laboratory. The polycrystalline sample of magnesium borohydride ammonia, $Mg(BH_4)_2(NH_3)_2$ (**I**), was loaded into a 1 mm thin-walled glass capillary under an inert atmosphere and sealed with vacuum grease. The capillary was mounted on a goniometer and was kept in constant rotation to average the crystallite statistics during the data collection. A Si(111) channel-cut monochromator selected a highly collimated incident X-ray beam. The diffracted X-rays were analyzed by reflection from a Ge(111) crystal and detected by a NaI scintillation counter.

Results and Discussion

Synthesis. The diammine complex **I** was prepared by desolvation of hexaammine complex $Mg(BH_4)_2 \cdot 6NH_3$ (**II**), which was synthesized by a method similar to that described in the literature,[8] based on the passing of gaseous ammonia through a solution of magnesium borohydride in ether (eq 1b). White sediment forms almost immediately at the contact of NH_3 with a solution of $Mg(BH_4)_2$. The filtration and drying in a vacuum at room temperature afforded a white solid with

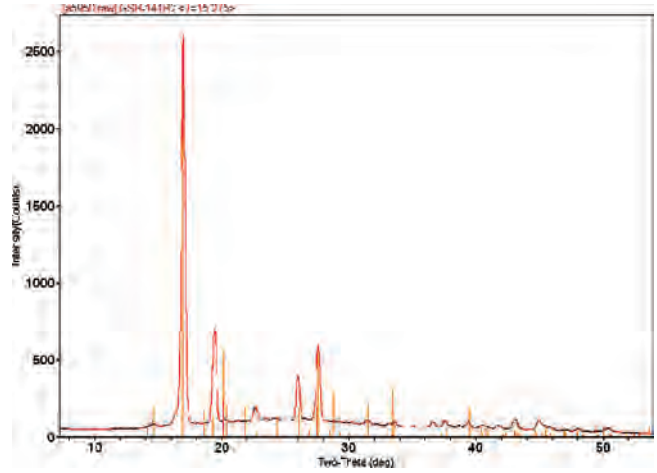

Figure 1. XRD patterns of the diammine complex of magnesium borohydride **I** (Cu Kα radiation). Tick marks indicate the location and integrated intensity of reflections for the phase calculated from high-resolution synchrotron powder diffraction data.

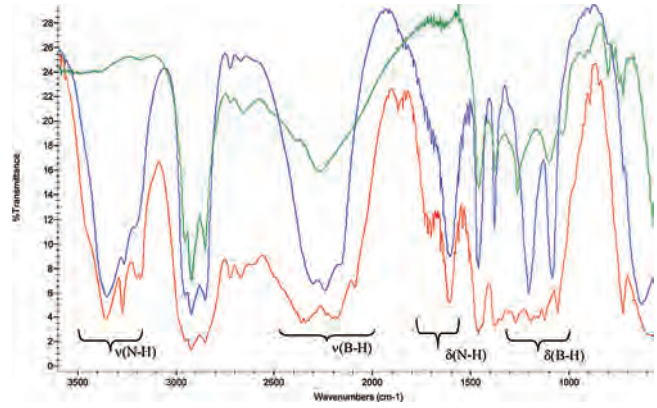

Figure 2. IR spectra of complexes **I** (red line) and **II** (blue line) compared with that of $Mg(BH_4)_2$ (green line).

composition $Mg(BH_4)_2 \cdot 6NH_3$. The complex **II** has been characterized by X-day diffraction, IR spectrum, and elemental analysis.

$$Mg(BH_4)_2 + 6NH_3 \rightarrow Mg(BH_4)_2 \cdot 6NH_3 \qquad (1b)$$

Decomposition of complex **II** in a vacuum at temperature 125 °C gives complex **I** (eq 2), which is a viscous colorless liquid at this temperature. It crystallizes into a white solid upon cooling. The NH_3:Mg ratio in **I** measured by elemental analysis is higher than 2 (usually 2.2−2.3) because of the possible incomplete decomposition of heaxaammine complex **II**. Despite the less than ideal elemental analysis, the powder XRD measurements showed the presence of only a single phase.

$$Mg(BH_4)_2 \cdot 6NH_3 \rightarrow Mg(BH_4)_2 \cdot 2NH_3 + 4NH_3 \qquad (2)$$

Complex **I** crystallizes in an orthorhombic lattice with parameters $a = 17.4872(4)$ Å, $b = 9.4132(2)$ Å, and $c = 8.7304(2)$ Å. Its XRD pattern is given in Figure 1. IR spectra of complex **I**, along with **II**, show bands assigned to N−H and B−H stretches (Figure 2). The B−H stretch band in complex **II** is symmetrical like the ones in the spectra of

(16) Hammersley, A. P. ESRF Internal Report ESRF98HA01T. FIT2D V9.129 Reference Manual V3.1; 1998.
(17) Chupas, P. J.; Ciraolo, M. F.; Hanson, J. C.; Grey, C. P. *J. Am. Chem. Soc.* **2001**, *123* (8), 1694–1702.

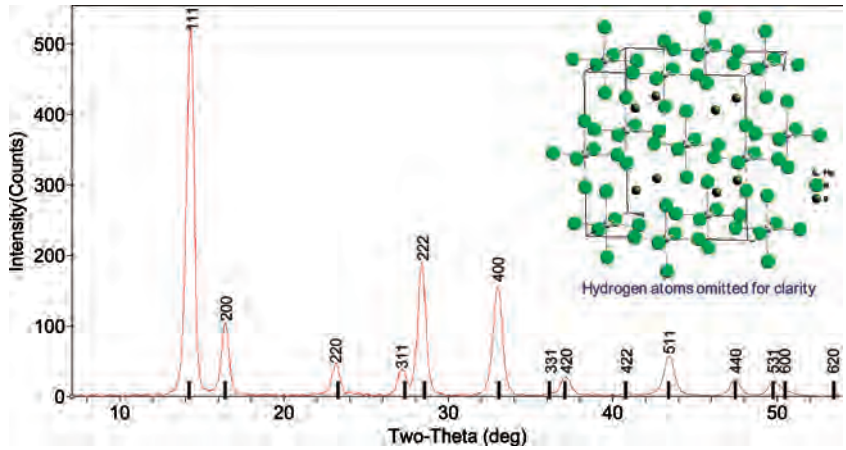

Figure 3. XRD pattern (indexed in a fcc cell with $a = 10.839$ Å) and the crystal structure (inset) of **II**. Mg atoms are in light gray, N atoms in green, and B atoms in gray. H atoms are omitted for clarity.

$NaBH_4$ and $Mg(BH_4)_2$[18] and indicates a high symmetry of the BH_4 tetrahedron. On the other hand, a broad band with two maxima in IR spectra of complex **I** indicates either a low-symmetry BH_4 group or the presence of two types of such groups in the structure. Similar IR spectra, with two maxima at about 2200 and 2420 cm^{-1}, were recorded for complexes $M(BH_4)_2 \cdot DG$ (DG = diglyme), where M = Mg and Ca but not Sr.[19] Later the single-crystal XRD analysis showed that $Ca(BH_4)_2 \cdot DG$ contains both bidentate and tridentate borohydride groups.[20]

Structure Determination. $Mg(BH_4)_2 \cdot 6NH_3$ (II). The XRD pattern of complex **II** is given in Figure 3. The face-centered-cubic (fcc) lattice, with parameter $a = 10.82(1)$ Å, is close to that found in $Mg(NH_3)_6Cl_2$, which crystallizes in an antitype of K_2PtCl_6.[21] The difference in the cell parameter (10.82 vs 10.19 Å) correlates with the difference in the ionic radii of BH_4^- and Cl^- anions.[22] Each Mg^{2+} atom is octahedrally coordinated to six NH_3 groups, while the BH_4^- (Cl^-) units occupy the ($^1/_4$, $^1/_4$, $^1/_4$) tetrahedral sites (Figure 3, inset). The quality of the diffraction data did not allow refinement to determine the H atom positions, but we expect that both the ammonia and borohydride H atoms are disordered around their respective central atoms (N and B, respectively). Our results are in disagreement with the orthorhombic cell reported for $Mg(BH_4)_2 \cdot 6NH_3$ in ref 13. Although we cannot completely rule out a small orthorhombic distortion, it is clear that our pattern does not fit the previously reported cell at ambient temperature ($a = 9.00$ Å, $b = 12.40$ Å, and $c = 10.78$ Å).[13]

$Mg(BH_4)_2 \cdot 2NH_3$ (I). The diffraction pattern of this phase was indexed by Topas-Academic[23] as orthorhombic, and space group *Pcab* was assigned based on systematic absences. A structure solution was found in space group *Pcab* (61) by the direct methods program, EXPO.[24] Rietveld refinement was performed using Topas-Academic. The Rietveld fit is shown in Figure 4, and refinement results are summarized in Table 1. Refined atomic coordinates are shown in Table 2. The quality of the data did not allow the independent determination of the H atoms; therefore, these were attached to the central B atom and the central N atom and treated as tetrahedral and pyramidal "rigid" bodies, with literature B−H and N−H distances of 1.20 and 1.00 Å, respectively. A penalty function was included to encourage Mg−H distances greater than 2.0 Å. Isotropic displacement parameters of H atoms were set to their corresponding B or N atoms. After the positions of the heavy atoms were refined, the orientations of the H tetrahedra and pyramids were determined by simulated annealing and then included in the refinement. It must be noted that powder XRD is much less sensitive to H atom positions than either single-crystal XRD or powder neutron diffraction (on deuterated samples). Therefore, the locations quoted in the refinement are more model-dependent than would be available from other techniques. Weakly restrained refinements of H atom positions retained the basic tetrahedral and pyramidal structures but led to negligible improvement in the quality of the fit. While the refinements were performed with a rigid-body treatment of the H atom positions, their estimated standard deviations (esd's) were computed from a full-matrix least-squares computation following refinement. It should be noted that, as is customary in reporting of crystallographic results, the esd's quoted in Table 2 come from the least-squares refinement and therefore measure uncertainty from the statistical errors in the data.[25] Realistic error estimates are several times larger for all atoms.

The structure of **I** is essentially molecular and built from pseudotetrahedral molecules $Mg(BH_4)_2 \cdot 2NH_3$ (Figure 5), in contrast to such ionic structures as $Mg(NH_3)_6(BH_4)_2$, $Mg(NH_3)_6Cl_2$,[21] or $Li_4BH_4(NH_2)_3$.[26,27] This structure is also

(18) Her, J.-H.; Stephens, P. W.; Gao, Y.; Soloveichik, G. L.; Rijssenbeek, J.; Andrus, M.; Zhao, J.-C. *Acta Crystallogr., Sect. B: Struct. Sci.* **2007**, *63* (4), 561–568.
(19) Titov, L. V.; Levicheva, M. D.; Psikha, S. B. *Zh. Neorg. Khim.* **1984**, *29* (3), 668–673.
(20) Lobkovskii, E. B.; Chekhlov, A. N.; Levicheva, M. D.; Titov, L. V. *Koord. Khim.* **1988**, *14* (4), 543–550.
(21) Olovsson, I. *Acta Crystallogr.* **1965**, *18* (5), 889–893.
(22) Pistorius, C. W. F. T. *Z. Phys. Chem. Neue Folge* **1974**, *88*, 253.
(23) Coelho, A. A. *Topas-Academic*; Bruker: New York, 2006.
(24) Altomare, A.; Burla, M. C.; Camalli, M.; Carrozzini, B.; Cascarano, G. L.; Giacovazzo, C.; Guagliardi, A.; Moliterni, A. G. G.; Polidori, G.; Rizzi, R. *J. Appl. Crystallogr.* **1999**, *32*, 339–340.
(25) Schwarzenbach, D.; Abrahams, S. C.; Flack, H. D.; Gonschorek, W.; Hahn, T.; Huml, K.; Marsh, R. E.; Prince, E.; Robertson, B. E.; Rollett, J. S.; Wilson, A. J. C. *Acta Crystallogr. Sect. A: Found. Crystallogr.* **1989**, *45* (1), 63–75.

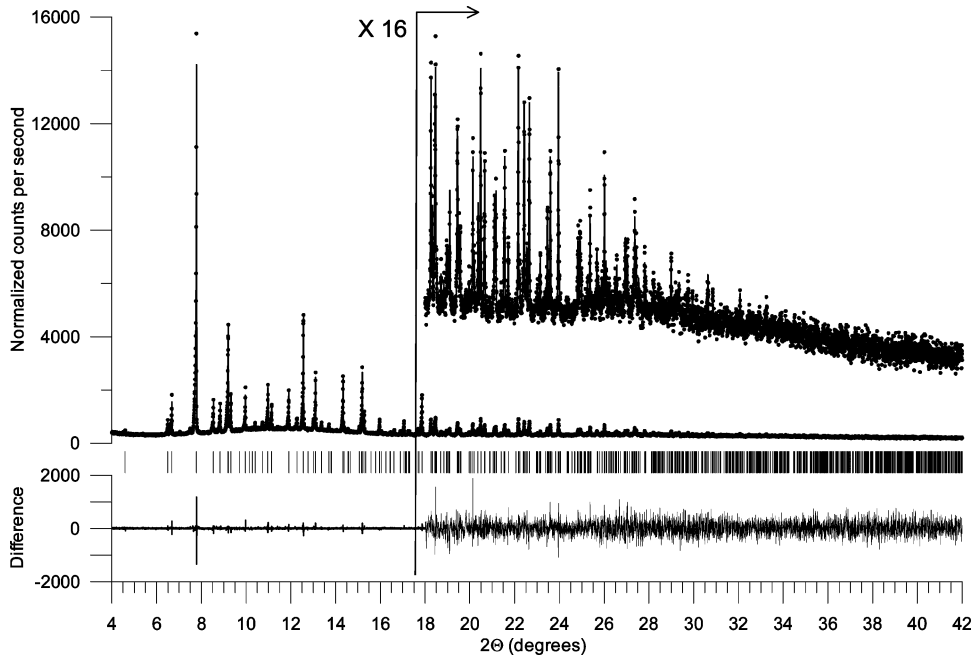

Figure 4. High-resolution synchrotron powder diffraction data (dots), Rietveld fit (line), and allowed Bragg reflections (tick marks) for **I**. The lower trace is the difference, $I_{meas} - I_{calc}$, on the same vertical scale.

Table 1. Experimental and Crystallographic Details for Complex **I**

Crystal Data	
chemical formula	$Mg(BH_4)_2(NH_3)_2$
M	88.05
cell setting, space group	orthorhombic, *Pcab*
data collection temperature (K)	298(2)
a, b, c (Å)	17.4872(4), 9.4132(2), 8.7304(2)
α, β, γ (deg)	90, 90, 90
volume (Å^3)	1437.1(1)
Z	8
D_x (computed, g/cm^3)	0.8139(1)
μ (cm^{-1})	1.0431
Data Collection	
diffractometer	X16C, NSLS, BNL
data collection method	specimen mounted in 1-mm-diameterrotating glass capillary; transmission mode; step scan
abs corrn	none
2θ (deg)	$2\theta_{min} = 2.000$, $2\theta_{max} = 42.000$, increment = 0.005
radiation type	synchrotron
wavelength of incident radiation (Å)	0.700 33(2)
specimen form, color	cylinder, white
specimen size (mm)	8 × 1 × 1
Refinement	
refinement method	Rietveld
excluded region(s)	none
profile function	Lorentzian line shape with computed axial divergence
no. of param	80
weighting scheme	$1/\sigma^2$
$(\Delta/\sigma)_{max}$	<0.001
H-atom treatment	tetrahedra centered on each B atom, pyramid with apical N atom
R_p	0.039
R_{wp}	0.049
R_{exp}	0.039
R_B	0.019
S (GOF, R_{wp}/R_{exp})	1.254
B−H distance	1.20 Å (fixed)
N−H distance	1.00 Å (fixed)

Table 2. Atomic Coordinates and B_{iso} Values of Complex **I**[a]

atom	x	y	z	B_{iso}
Mg1	0.62298(17)	0.15583(20)	0.46634(17)	3.71(7)
N2	0.52544(54)	0.29429(85)	0.47670(76)	5.1(1)
H2a	0.5282(38)	0.3531(68)	0.5719(71)	5.1(1)
H2b	0.5252(33)	0.3580(86)	0.3850(63)	5.1(1)
H2c	0.4776(44)	0.2362(67)	0.4780(76)	5.1(1)
N3	0.70955(47)	0.28597(78)	0.53200(86)	5.1(1)
H3a	0.6961(35)	0.3324(66)	0.6314(69)	5.1(1)
H3b	0.7574(52)	0.2291(60)	0.5449(75	5.1(1)
H3c	0.7178(34)	0.3605(80)	0.4520(68)	5.1(1)
B4	0.63702(63)	0.0861(10)	0.2121(11)	3.7(2)
H4a	0.6340(43)	0.2126(56)	0.2281(18)	3.7(2)
H4b	0.6534(29)	0.0588(63)	0.0819(54)	3.7(2)
H4c	0.5760(31)	0.0350(59)	0.2421(63)	3.7(2)
H4d	0.6847(33)	0.0380(21)	0.2963(22)	3.7(2)
B5	0.60569(58)	0.97026(84)	0.6607(11)	3.7(2)
H5a	0.6692(30)	0.9833(19)	0.6106(53)	3.7(2)
H5b	0.5982(29)	0.0453(53)	0.7708(63)	3.7(2)
H5c	0.5953(27)	0.8488(58)	0.6969(56)	3.7(2)
H5d	0.5600(9)	0.0037(22)	0.5645(25)	3.7(2)

[a] esd's are statistical values from the Rietveld refinement as discussed in the text. The angular esd's for the rigid polyhedra are the following: along axes a, b, and c respectively for N-centered pyramids 0.11°, 0.12°, and 0.14°, for the tetrahedron centered at the B4 atom 1.40°, 1.56°, and 1.68°, and for the tetrahedron centered at the B5 atom 0.79°, 0.72°, and 1.50°.

different from polymeric structures of halide complexes $Mg(NH_3)X_2$ (X = Cl, Br, and I), which have chains of edge-sharing octahedra with bridged halogen atoms and ammonia ligands in the trans position.[28] The average Mg−N distance in **I** (2.09 Å) is practically the same as those in $Mg(NH_3)_2Cl_2$, $Mg(NH_3)_2Br_2$, and $Mg(NH_3)_2I_2$ (2.130, 2.118, and 2.119 Å, respectively).[28] The Mg−N distances in ionic hexacoordinated ammine magnesium complexes $Mg(NH_3)_6Cl_2$ (2.197 Å) and $Mg(NH_3)_6Hg_{22}$ (2.205 Å) are noticeably longer.[29]

(26) Filinchuk, Y. E.; Yvon, K.; Meisner, G. P.; Pinkerton, F. E.; Balogh, M. P. *Inorg. Chem.* **2006**, *45* (4), 1433–1435.
(27) Chater, P. A.; David, W. I. F.; Johnson, S. R.; Edwards, P. P.; Anderson, P. A. *Chem. Commun.* **2006**, (23), 2439–2441.
(28) Leineweber, A.; Friedriszik, M. W.; Jacobs, H. *J. Solid State Chem.* **1999**, *147* (1), 229–234.
(29) Hwang, I. C.; Drews, T.; Seppelt, K. *J. Am. Chem. Soc.* **2000**, *122* (35), 8486–8489.

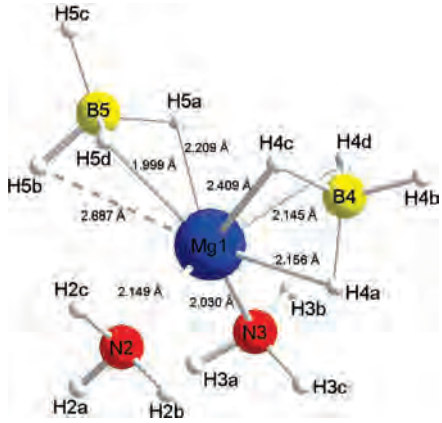

Figure 5. Molecular structure of complex **I**.

The difference in the structures of these complexes is evidently not caused by steric factors (the ionic radius of the BH_4^- group is close to that of Br^-) but rather the tendency of halide atoms to form bridging M−X−M bonds. The BH_4^- anion is a much weaker Lewis base than the unshared electron pair of a halogen atom. Therefore, bridging borohydride groups, though rather common in polymer borohydrides of light elements like $Be(BH_4)_2$,[30] are very rare in molecular complexes and are found only in binuclear complexes of lanthanides $[(C_5H_3{}^tBu_2)_2Ln(\mu\text{-}BH_4)]_2$ (Ln = Ce[31] and Sm[32]) and manganese $Mn_2(\mu\text{-}BH_4)(\mu\text{-}H)(CO)_5(\mu\text{-}dppe)$[33] and in polymer structures of $Be(BH_4)_2$ with helical polymeric $BeH_2BH_2BeH_2BH_2$ chains[30] and $Mg(BH_4)_2$ with a complex 3D structure.[18,34]

The closest molecular analogue of **I** is a monomeric complex $Mg(BH_4)_2 \cdot$TMEDA (**III**)[35] with the same N_2B_2 pseudotetrahedral coordination of the Mg atom. However, two borohydride groups in **I** are different and bound to the Mg atom via three Mg−H−B4 bonds (tridentate coordination) and two Mg−H−B5 bonds (bidentate coordination) (Figure 5 and Table 3). Tridentate borohydride groups were found in a few other magnesium borohydride complexes: **III**[35] and dimeric $[Mg(BH_4)(\mu\text{-}OR)L]_2$, where R = ^{i}Pr, $_t$Bu, CH_2CMe_3, $SiMe_3$, and Ph and L = THF and Et_2O.[36] The Mg···B4 distance in **I** (2.33 Å) is close to the high limit of the range found in complexes with tridentate BH_4 groups (2.25−2.32 Å)[35,36] but shorter than that found in magnesium borohydride complexes with three donor atoms $Mg(BH_4)_2 \cdot 3L$ (L = THF,[37] N^tBuH_2, and HNC_5H_{10}[38]) and $Mg(BH_4)_2 \cdot DG$[39] (2.40−2.55 Å) and unsolvated $Mg(BH_4)_2$[18] (2.41−2.45 Å) with bidentate borohydride groups, while the Mg···B5 distance (2.454 Å) is exactly in this range. This difference in coordination of two borohydride groups correlates with IR data. Both types of coordination supposedly exist in the ionic salt $(PPh_4)_2[Mg(BH_4)_4]$ with two crystallographically independent BH_4 groups.[40] However, the Mg···B distances in this anion are almost equal (2.42 and 2.43 Å), and their lengths are close to the distance in complex $Mg(BH_4)_2 \cdot 3THF$ with bidentate borohydride groups (2.44 Å),[37] which suggests only bidentate bonding in $(PPh_4)_2[Mg(BH_4)_4]$. It should be noted that in most bidentate BH_4 groups the metal atom, boron, and the two bridging H atoms lie in the same plane but in **I** boron atom B5 is pulled out of the plane. This can be explained by participation of hydrogen atom H5c in the H···H interactions (Figure S1 in the Supporting Information).

Table 3. Selected Interatomic Distances (Å) and Angles (deg) in the Crystal Structure of **I**

distance		angle	
Mg1−N2	2.149(5)	N2−Mg1−N3	102.36(14)
Mg1−N3	2.030(5)	B4···Mg1···B5	118.14(14)
Mg1···B4	2.328(3)		
Mg1···B5	2.454(4)		
Mg1−H4a	2.16(3)		
Mg1−H4c	2.41(3)		
Mg1−H4d	2.15(3)		
Mg1−H5a	2.21(2)		
Mg1−H5b	2.89(2)		
Mg1−H5d	2.00(2)		

The average $Mg-H^b$ distance [2.19(8) Å excluding the outlier Mg−H5b] is close to the value found in **III** (2.10 Å),[35] unsolvated magnesium borohydride (average 2.0 Å),[18] and other magnesium borohydride complexes (1.97−2.14 Å). Though H atom positions from powder XRD data could not be refined independently and so this result is somewhat model-dependent, the combination of chemical properties, low rotational esd's of the rigid NH_3 and BH_4 polyhedra and realistic atomic esd's of H and non-H atoms (Table 2), reasonable values of Mg−H distances, and peculiar crystal packing motif (vide infra) will all lend credence to the proposed bonding structure of complex **I**.

An interesting theoretical and practical question is whether N−H···H−B dihydrogen bonds exist in the solid phase of **I**. In solid ammonia borane, BH_3NH_3, it seems that the presence of such bonds and, therefore, the close proximity of N and B atoms direct its decomposition predominantly to hydrogen and products with N−B bonds.[5] $Mg(BH_4)_2 \cdot 2NH_3$ molecules in **I** are packed in a such way that the N_2 edge of one molecule faces one B atom of another molecule (Figure 6a). These interactions lead to the arrangement of the $Mg(BH)_4 \cdot 2NH_3$ molecules into slabs perpendicular to the *a* axis. The slabs then stack in an AABBAABB... fashion wherein the A and B slabs are rotated 180° with respect to each other in the *bc* plane (Figure 6b). The shortest H···H distances in intermolecular N−H···H−B bonds in **I** (Table

(30) Lipscomb, W. N.; Marynick, D. *J. Am. Chem. Soc.* **1971**, *93* (9), 2322–2323.
(31) Lobkovsky, E. B.; Gun'ko, Y. K.; Bulychev, B. M.; Belsky, V. K.; Soloveichik, G. L.; Antipin, M. Y. *J. Organomet. Chem.* **1991**, *406* (3), 343–352.
(32) Gun'ko, Y. K.; Bulychev, B. M.; Soloveichik, G. L.; Bel'skii, V. K. *J. Organomet. Chem.* **1992**, *424* (3), 289–300.
(33) Carreno, R.; Riera, V.; Ruiz, M. A.; Bois, C.; Jeannin, Y. *Organometallics* **1993**, *12* (5), 1946–1953.
(34) Cerný, R.; Filinchuk, Y.; Hagemann, H.; Yvon, K. *Angew. Chem., Int. Ed.* **2007**, *46* (30), 5765–5767.
(35) Soloveichik, G. L.; Andrus, M.; Lobkovsky, E. B. *Inorg. Chem.* **2007**, *46* (10), 3790–3791.
(36) Bremer, M.; Linti, G.; Noeth, H.; Thomann-Albach, M.; Wagner, G. E. W. J. *Z. Anorg. Allg. Chem.* **2005**, *631* (4), 683–697.
(37) Noeth, H. *Z. Naturforsch., B: Anorg. Chem., Org. Chem.* **1982**, *37B* (12), 1499–1503.
(38) Bremer, M.; Nöth, H.; Warchhold, M. *Eur. J. Inorg. Chem.* **2003**, *2003* (1), 111–119.
(39) Lobkovskii, E. B.; Titov, L. V.; Levicheva, M. D.; Chekhlov, A. N. *J. Struct. Chem.* **1990**, *31* (3), 506–508.
(40) Makhaev, V. D.; Borisov, A. P.; Antsyshkina, A. S.; Sadikov, G. G. *Zh. Neorg. Khim.* **2004**, *49* (3), 371–379.

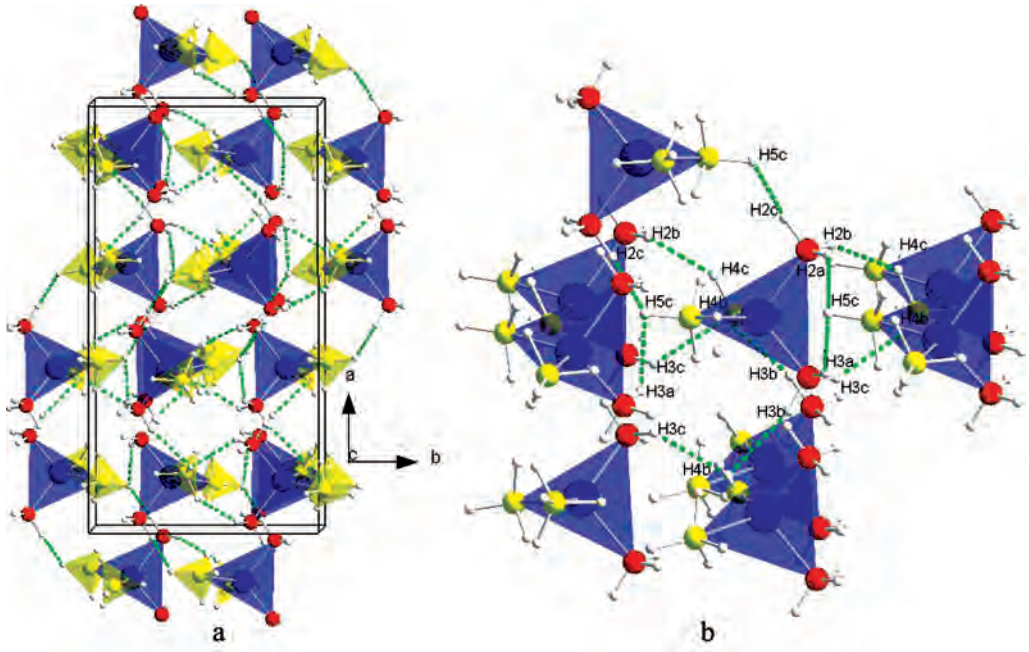

Figure 6. Molecular packing (a) and network of N−H···H−B dihydrogen bonds (b) in crystal **I**. Mg atoms are in blue, N atoms in red, B atoms in yellow, and H atoms in white. H···H interactions of less than 2.33 Å are shown as dashed green lines.

Table 4. Interatomic Distances (Å) and Angles (deg) for Apparent Dihydrogen Bonds in **I**

distance		angle		angle	
H4b···H3b	2.26(4)	B4−H4b···H3b	98.6(16)	N3−H3b···H4b	166.8(29)
H4b···H3c	2.20(5)	B4−H4b···H3c	115.6(17)	N3−H3c···H4b	128.0(30)
H4c···H2b	2.19(4)	B4−H4c···H2b	123.7(19)	N2−H2b···H4c	149.3(28)
H5c···H2c	2.14(4)	B5−H5c···H2c	105.0(12)	N2−H2c···H5c	134.0(29)
H5c···H3a	2.32(3)	B5−H5c···H3a	96.8(14)	N3−H3a···H5c	140.3(62)

4) are in the range 2.2−2.3 Å, which is apparently longer than that found in compounds with more reliably determined dihydrogen bonds (1.7−2.2 Å). However, the average N−H···H and B−H···H angles in **I** (144° and 108°) appear to be similar to those found in the most accurate structure of BH_3NH_3 determined by neutron diffraction (156° and 106°, respectively). These values for apparent dihydrogen bonds, though based on not truly imaged individual H atoms, are in good correlation with the overall structure.

Theoretical calculations using MP2 of dimers of ammonia borane BH_3NH_3, aminoborane BH_2NH_2, and ammonia[41] showed that the energy of the dihydrogen bond in $(BH_3NH_3)_2$ is higher than that of the classical hydrogen bond in ammonia, and the calculated N−H···H angle (149°) is comparable to that found in solid BH_3NH_3.[4] Similar N−H···H−B dihydrogen bonds were found in the crystal structure of another borohydride ammine complex, $Al(BH_4)_2 \cdot NH_3$.[42] These N−H···H−B dihydrogen bonds define its crystal structure by linking individual molecules into spiral chains via two such bonds, while the third bond connects the chains into layers.[42] The shortest intermolecular N···B distances in this complex (3.5−3.6 Å) are very close to those found in **I** (3.56−3.70 Å). By comparison, the B−N interatomic distances in ionic complex **II** are much longer (approximately 3.9 Å), which suggests no interaction between NH_3 and BH_4^- groups.

The main motif of the network of apparent dihydrogen bonds in **I** is bonding between the terminal H atom of each BH_4 group and two H atoms from adjacent ammonia ligands with the shortest H···H distances (Table 4). These bonds are complemented with dihydrogen bonds with participation of bridge hydrogen atom H4b of the tridentate BH_4 group (that is reflected in the elongation of the Mg−H bond to 2.4 vs 2.1−2.2 Å). This atom is connected only with one H atom of the ammonia ligands. All H atoms in the N3 ligand are connected to hydride H atoms, but only two participate in H−H bonding in the N2 ligand. This difference correlates with the difference in the Mg−N bond lengths (Table 3).

Thermal Decomposition of Ammine Complexes of Magnesium Borohydride. It was reported that hydrogen is the major product at decomposition of $Mg(BH_4)_2 \cdot 2NH_3$.[8] Therefore, complex **I** may be a valuable material for hydrogen storage. We studied the thermal decomposition of complexes **I** and **II** using TPD, DSC, and in situ XRD methods. DSC of complex **II** at a rate of 10 °C/min results in an endothermic effect starting at 80 °C (Figure 7), which corresponds to evolution of ammonia as found by its condensation in a cold trap. The major endothermic peak with its onset at 128 °C and its maximum at 172 °C corresponds to evolution of both ammonia and hydrogen.

(41) Kar, T.; Scheiner, S. *J. Chem. Phys.* **2003**, *119* (3), 1473–1482.
(42) Lobkovskii, É.; Polyakova, V.; Shilkin, S.; Semenenko, K. *J. Struct. Chem.* **1975**, *16* (1), 66–72.

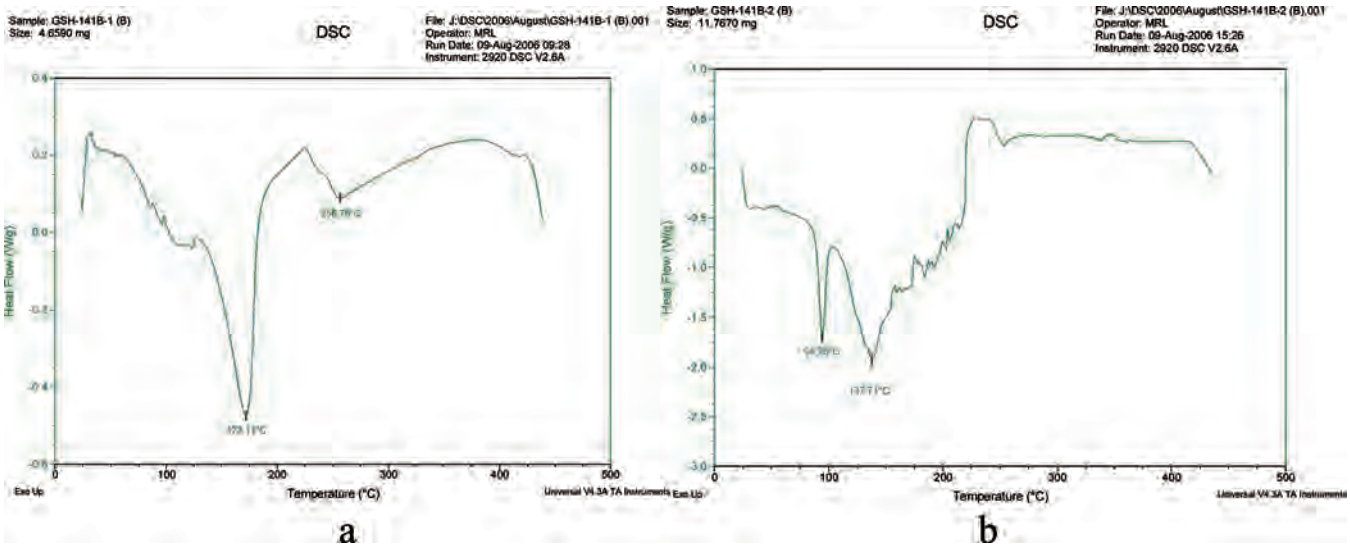

Figure 7. DSC heating curves of complexes **II** (a) and **I** (b).

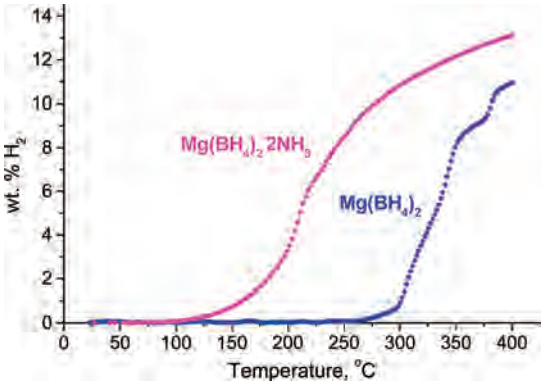

Figure 8. Gas evolution from complex **I** (magenta line) and $Mg(BH_4)_2$ (blue line). The vertical axis calibration as weight percent H_2 is based on the assumption that all evolved gas is hydrogen.

Therefore, this regime cannot be used either for hydrogen generation or for desolvation of **II** to form **I**. However, the heating of complex **II** in a dynamic vacuum at 100−125 °C yields diammine complex **I**.

DSC of samples of complex **I** shows a sharp endothermic effect at 94 °C (Figure 7b) that corresponds to melting. This assignment was confirmed visually and by the disappearance of the diffraction pattern during in situ XRD experiments above 90 °C. The endothermic peak at 137 °C, associated with hydrogen evolution, has distinct "wiggles" that are observed when a liquid forms a foam with a solid "crust", preventing gas ventilation.

TPD measurements (Figure 8) showed the onset of gas evolution for complex **I** around 120 °C (above the melting point) and reaching a maximum rate at around 200 °C. It seems that decomposition of **I** takes place in two distinct stages with approximately equal amounts of released hydrogen. The second stage started at about 220 °C and was almost complete by the time the sample reached 400 °C. A total of 13.1 wt % H_2 was released at this temperature (assuming that all of the desorbed gas is hydrogen), which is less than the theoretical 16.0 wt % (Figure 8). At the same temperature and heating rate, magnesium borohydride released only 10.9 wt % H_2 (Figure 8) and its decomposition started at about 280 °C. These data differ from those reported by Konoplev and Silina,[8] but because no purity (elemental analysis) or XRD data were given in this reference, it is possible that these are different materials.

Residual gas analysis (RGA) during desorption registered some ammonia evolution at a level at least 2 orders of magnitude lower than that of hydrogen. This is not surprising given that elemental analysis indicated the presence of higher ammine complexes [e.g., $Mg(NH_3)_6(BH_4)_2$, which evolves ammonia at <125 °C]. It is also possible that NH_3 is released along with hydrogen evolution from the diammine complex. Indeed, we registered some sample weight loss in excess of hydrogen release measured by TPD (up to 5−7%). This "non-hydrogen" weight loss may be attributed to ammonia or to the escape of a part of the sample during foaming from the sample vial, which we observed. Even if we assume that all of the weight loss is due to ammonia release, it will only slightly reduce the hydrogen content (up to 0.8%).

As in the case $LiBH_4$, decomposition of **I** occurs from the liquid phase and no crystalline products were found up to 350 °C by in situ XRD experiments. It should be noted that the amount of hydrogen released during thermal decomposition up to 400 °C is less than the theoretical value (13.1% vs 16.0%). A possible explanation is the formation of stable intermediate compounds containing B−H bonds like the $B_{12}H_{12}^{2-}$ anion, which was proposed to form during decomposition of $LiBH_4$[43] and recently found by ^{11}B NMR during thermal decomposition of several metal borohydrides including $Mg(BH_4)_2$.[44] Indeed, TPD of the sample of complex **I** to 500 °C releases 14.9% (assuming all hydrogen), and continued heating at this temperature with periodic evacuation of the sample chamber raises the total amount to 15.9%.

(43) Zuttel, A.; Rentsch, S.; Fischer, P.; Wenger, P.; Sudan, P.; Mauron, P.; Emmenegger, C. *J. Alloys Compd.* **2003**, *35* (6357), 515–520.
(44) Hwang, S.-J.; Bowman, B. C., Jr.; Reiter, J. W.; Rijssenbeek, J. R.; Soloveichik, G. L.; Zhao, J.-C.; Kabbour, H.; Ahn, C. C. *J. Phys. Chem. C* **2008**, *112*, 3164–3169.

The only crystalline phase detected by XRD in a sample heated to 500 °C is a small amount of BN. The presence of BN as a decomposition product suggests that decomposition, at least partially, may occur via reaction (3).

$$Mg(BH_4)_2 \cdot 2NH_3 \rightarrow MgH_2 + 2BN + 6H_2 \quad (3)$$

However, in contrast to the decomposition of $Mg(BH_4)_2$, neither MgH_2 nor its decomposition product, Mg, which are usually well-crystallized, was found as a decomposition product. It is possible that the main decomposition pathway of **I** ultimately yields magnesium boronitrides Mg_3BN_3 or $Mg_3B_2N_4$ (known catalysts for the synthesis of cubic boron nitride)[45] along with BN and amorphous boron (eq 4), probably via intermediate formation of polyborane anions or polymeric [MgN2(BH)2]x.

$$3Mg(BH_4)_2 \cdot 2NH_3 \rightarrow Mg_3B_2N_4 + 2BN + 2B + 21H_2 \quad (4)$$

Attempts to recharge the decomposition products of **I** at 250 °C and 5.9 MPa (60 bar) of H_2 for up to 60 h were unsuccessful. No crystalline phases, such as the anticipated MgH_2, were observed after exposure to hydrogen pressure.

Conclusion

Our study of $Mg(BH_4)_2 \cdot 2NH_3$ was prompted by its potential use as a hydrogen storage material. Its structure is built from independent molecules $Mg(BH_4)_2 \cdot 2NH_3$ packed into a layered crystal structure, evidently mediated by formation of N−H···H−B dihydrogen bonds. The relatively low hydrogen desorption temperature and high hydrogen capacity make $Mg(BH_4)_2 \cdot 2NH_3$ a compelling candidate for hydrogen storage competitive with ammonia borane, which suffers from the same problem with hydrogen purity. In contrast to BH_3NH_3, thermal decomposition of **I** is endothermic, which makes the hydrogen release process controllable and potentially more readily reversible. It remains possible that traces of ammonia found in the gas phase during the decomposition process are the result of higher ammine complex impurities. Therefore, it is necessary to develop a synthesis method for pure **I** with an exact Mg/B/N ratio of 1:2:2. Clearly, ammonia release during decomposition must be prevented and reversibility achieved for this material to become practical.

Acknowledgment. The authors acknowledge valuable technical assistance from Tom Raber, Sergei Kniajanski, and Maria LaTorre at GE Global Research and Jonathan Hanson at Brookhaven National Laboratory. Use of the National Synchrotron Light Source, Brookhaven National Laboratory, was supported by the U.S. Department of Energy (DOE), Office of Science, Office of Basic Energy Sciences, under Contract No. DE-AC02-98CH10886. Part of the work was supported by DOE, Office of Energy Efficiency and Renewable Energy, under Contract No. DE-FC3605GO15062 as part of the DOE Metal Hydride Center of Excellence.

Supporting Information Available: X-ray crystallographic data in CIF format and a diagram of the tilting of the bidenatate BH_4 group in complex **I**. This material is available free of charge via the Internet at http://pubs.acs.org.

IC7023633

(45) B−Mg−N (Boron−Magnesium−Nitrogen). *Light Metal Systems*; Materials Science International Team: Springer, Berlin, 2006; Part 4, pp 1−17.